DOI: 10.1002/ejoc.200800811

Anion Recognition by Neutral Macrocyclic Azole Amides

Markus Schnopp,[a] Silvia Ernst,[a] and Gebhard Haberhauer*[a]

Keywords: Anions / Host–guest systems / Hydrogen bonds / Macrocyclic ligands / Receptors

A straightforward synthesis of C_2-symmetric azole-containing macrocyclic peptides is presented. This type of macrocycle possesses four amide groups directed into the interior of the scaffold that act as hydrogen-bond donors and two nitrogen atoms from the azole unit that act as hydrogen-bond acceptors. This arrangement makes them sensitive receptors for Y-shaped anions like AcO^- and $H_2PO_4^-$ with a selectivity for dihydrogen phosphate versus acetate, as was shown with ^1H NMR titration techniques in [D_6]DMSO/5 % $CDCl_3$.

Introduction

The design and synthesis of new systems for selective anion recognition is an emerging field in supramolecular chemistry,[1–3] as noncovalent anion interaction plays an important role in many essential biological, chemical and environmental processes.[4] A key problem herein is the design of synthetic receptors with convergent binding groups that are arranged to match the functionality of the guest molecule. Such receptors are not only to show high affinity, but also high selectivity, as this is important for sensing applications. Many anions like acetate, phosphate or sulfate anions have different geometric structures, which open up possible routes to the development of shape-selective anion receptors. Examples of natural receptors binding strongly and effectively phosphate or sulfate anions in water indicate that there is a potential for further improvements.[5] In these receptors, amide groups with their intrinsic ability to form hydrogen bonds play an important role. Therefore, the study of amide-based recognition systems appears particularly interesting. The directional character and the relatively small strength of individual hydrogen bonds requires the active cooperation of multiple, precisely positioned hydrogen-bond donor groups in the host structure in order to achieve strong and selective complexation with anionic guests.[6,7]

Recently, we developed novel macrocyclic azole-containing ligands based on the structural motif of *Lissoclinum* cyclopeptide alkaloids as receptors for neutral guest molecules,[8] for the control of axial and planar chirality[9,10] and for chirality transfer in C_3-symmetric compounds.[11,12] In these systems, the amide groups of the macrocyclic ligands are primarily used to connect the azole units with each other and to reduce the possible number of conformers of the macrocyclic rings. The valine–azole subunits in these macrocycles show, similarly to 2,6-pyridinediamides, strong preference for a *syn–syn* conformation of both amide NH groups.[13,14] This *syn–syn* preference results from hydrogen bonding with the azole nitrogen atom (Figure 1). The alternative conformations (*syn–anti* and *anti–anti*) are disfavoured due to lone pair repulsion. As a result, the azole subunit is rigid and shows two hydrogen-bond donation groups in a common direction, and therefore, it should be able to strongly bind anions.

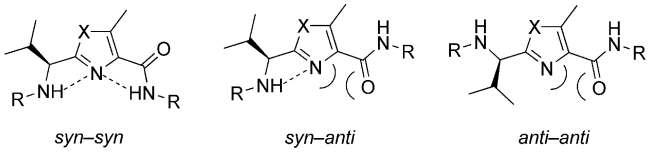

Figure 1. Conformations of the valine–azole subunits.

Our intention was to develop efficient receptors for Y-shaped anions such as acetate and phosphate in polar solvents. Therefore, we decided to study C_2-symmetric recep-

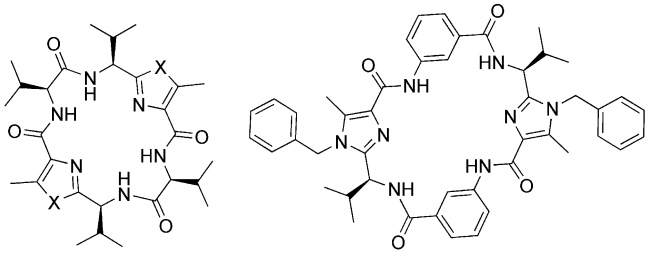

Figure 2. Structures of the azole-containing C_2-symmetric macrocyclic receptors.

[a] Institut für Organische Chemie, Fachbereich Chemie, Universität Duisburg-Essen,
Universitätsstraße 7, 45117 Essen, Germany
E-mail: gebhard.haberhauer@uni-due.de

tors consisting of two valine–azole subunits linked with valine units and *meta*-aminobenzoic acid moieties (Figure 2). Herein we report the synthesis of the azole-containing C_2-symmetric receptors **2**–**4** and the anion binding properties of **1**–**4** by using ^{1}H NMR titration techniques.

Results and Discussion

Synthesis of the Receptors

The synthesis of receptors **2** and **3** was conducted in analogy to the straightforward synthesis of macrocycle **1**[9] (Scheme 1). The starting materials for all receptors are the corresponding azoles **5**. Saponification of methyl esters **5** with NaOH in a mixture of MeOH/dioxane afforded azole acids **6** in almost quantitative yield. Without further purification, azole carboxylic acids **6** were coupled by using pentafluorophenyl diphenylphosphinate (FDPP) and *N*-ethyldiisopropylamine in absolute CH_3CN at room temperature with readily available (L)-valine *tert*-butyl ester hydrochloride (**7**) in very high yields (89 to 98%). The so-received valine–azole building blocks **8** can be deprotected on both sides by stirring in a solution of HCl in ethyl acetate or by using a large excess of trifluoroacetic acid (TFA) in dichloromethane. In a final step, free amino acids **9** were dimerized under high-dilution conditions. The best yields (up to 48%) were obtained by using FDPP as the coupling reagent in the presence of *N*-ethyldiisopropylamine.

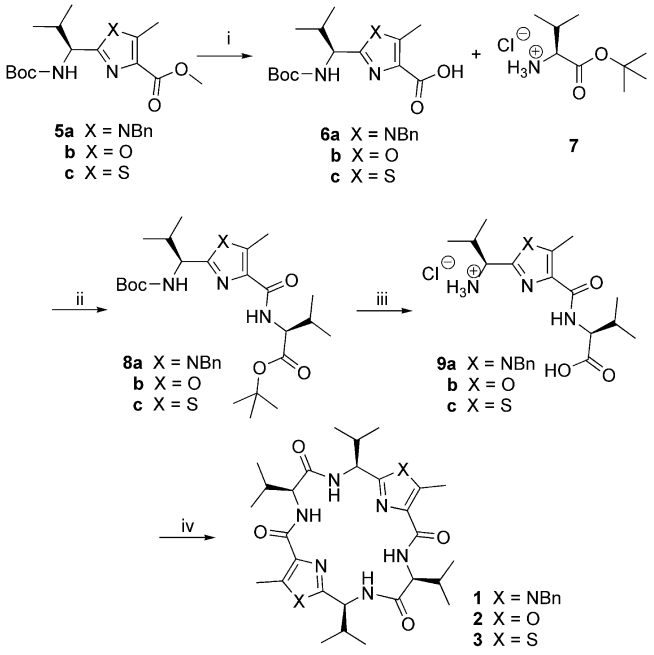

Scheme 1. Synthesis of receptor **1**–**3**. Reagents and conditions: (i) 2 M NaOH, MeOH/dioxane, 0 °C → r.t., 99%; (ii) FDPP, *i*Pr_2NEt, CH_3CN, r.t., 89% for **8a**, 94% for **8b** and 98% for **8c**; (iii) HCl, EtOAc, quant.; (iv) FDPP, *i*Pr_2NEt, CH_3CN, r.t., 45% for **1**, 48% for **2** and 19% for **3**.

Larger receptor **4** was prepared in an analogues manner (Scheme 2). Imidazole carboxylic acid **6a** was coupled by using FDPP in CH_3CN to commercially available methyl 3-aminobenzoate (**10**) to afford building block **11**. This coupling required uncommonly long reaction times (1 week at room temperature) to obtain acceptable yields of the products (41% for **11**), which is the result of the lower nucleophilicity of aniline **10** relative to that of amine **7**. Deprotection of the carboxyl residue by saponification afforded acid **12**. Subsequent removal of the Boc group provided free amino acid **13**, which was submitted to a cyclodimerization with FDPP to give receptor **4** in a good yield of 52%.

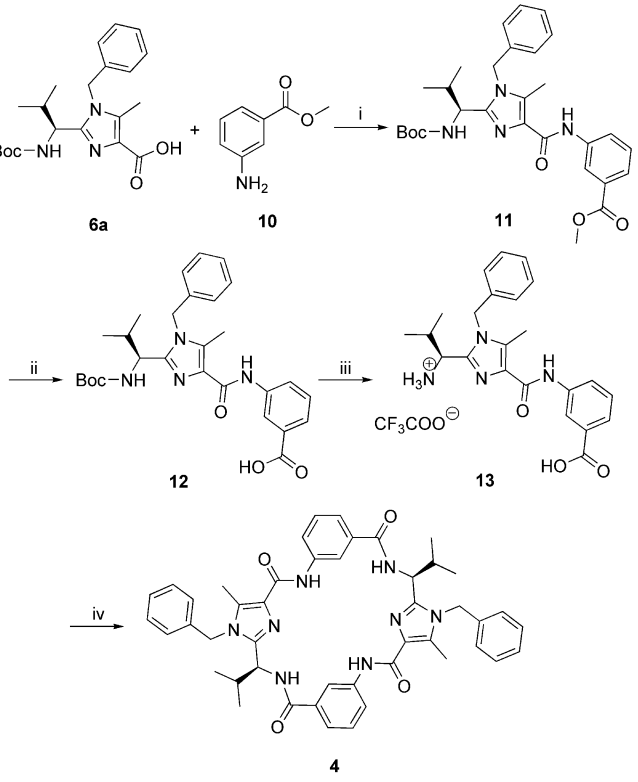

Scheme 2. Synthesis of receptor **4**. Reagents and conditions: (i) FDPP, *i*Pr_2NEt, CH_3CN, r.t., 41%; (ii) 2 N NaOH, MeOH/dioxane, 0 °C → r.t., quant.; (iii) TFA, DCM, 0 °C → r.t., quant.; (iv) FDPP, *i*Pr_2NEt, CH_3CN, r.t., 52%.

Structural Investigations

The NMR spectra of cyclic peptides **1**–**4** are consistent with a C_2-symmetric structure in solution. The vicinal $^3J_{HN,CH}$ values of 7.2–10.3 Hz for **1**–**4** correspond to dihedral angles of $145° < |\theta| < 180°$ in the macrocycle.[15]

The structures of azole-based cyclic amides **1**–**4** in the gas phase were investigated by molecular modelling studies by using the Gaussian software program.[16] To determine the preferred conformation of the cycles, we performed full geometry optimization by applying the DFT-B3LYP method and by using the 6-31G* basis set. A comparison of the calculated structure data of azole amides **1**–**3** shows that they exhibit essentially the same structure. This is in contrast to the known C_2-symmetric azole macrocycles where the structural type depends on the type of the azole unit.[17] The valine–azole subunits in macrocycles **1**–**4** have

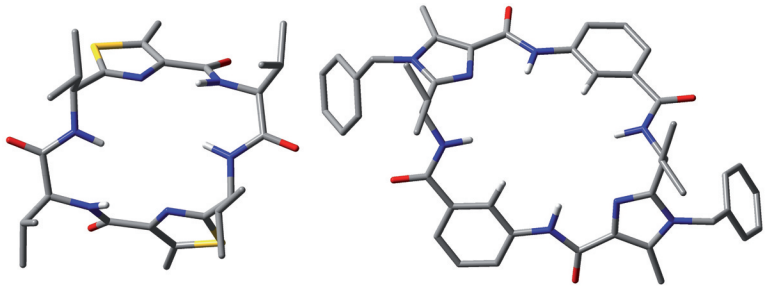

Figure 3. Molecular structures of the energetically preferred conformers of **3** and **4** calculated by using B3LYP/6-31G*; all hydrogen atoms except those pointing into the interior of the macrocycles are omitted for clarity.

syn–syn conformations for both amide NH groups, and the (L)-valine side chains are all directed from the same face of the macrocycle. The four hydrogen atoms of the amides and the electron pairs of the azole nitrogen point into the interior of the macrocycle (Figure 3). All dihedral angles χ [N_{amide}–C_{α}–C_{azole}–X_{azole}] of macrocycles **1**–**3** are approximately 100°, and the distance between the tertiary nitrogen atoms of the azole rings is between 4.5 and 4.7 Å.

The interior of macrocycle **4** is larger; here, the distance between the tertiary nitrogen atoms of the azole rings is calculated to be 7.1 Å. Here again, the four hydrogen atoms of the amides point into the interior of the macrocycle. Therefore, the NH groups are perfectly arranged in a corporate direction, which should result in a strong binding of anions through hydrogen bonding.

Anion Binding

For investigating the stability of the complexes of receptors **1**–**4** and anions we applied standard ^{1}H NMR titration experiments, as NMR spectroscopy is one of the most effective tools to study host–guest supramolecular chemistry. By adding guest molecules to the ligands, the signals in the ^{1}H NMR spectra migrate upfield or downfield as a result of the interactions between the hydrogen-bond donor and acceptor. From the extent of these shifts, conclusions can be drawn as to which individual protons are involved in the interaction, as well as to the extent to which they participate.[18,19] As solvent, we decided to use DMSO, which with its strong hydrogen-acceptor properties of the oxygen is able to act as a strong competitor for hydrogen-bond donor sites in a receptor. In the case of very good anion receptors, the use of apolar solvents like $CDCl_3$ would result in binding constants higher than 10^5 M^{-1}, which goes beyond the limit of the NMR technique. A further reason to perform NMR titrations in DMSO is the fact that this method is commonly used in the literature and comparisons to other anion receptors can readily be made. Nevertheless we added 5% of $CDCl_3$, because the solubility of the receptors in pure DMSO was too low.

For the measurements we used a constant host concentration (1×10^{-3} M) and increased the concentration of the anions (0.2–10 equiv.). We could observe significant downfield shifts of the amide signals, which indicate the hydrogen-bonding interactions. Furthermore, the spectra show a fast equilibrium between free and complexed forms of the ligands. Standard nonlinear analysis of the chemical shift data delivered the 1:1 binding constants for receptors **1**–**4**, which are summarized in Table 1. To confirm the 1:1 stoichiometry, Job plots for complexation of receptor **3** and the TBA salts of dihydrogen phosphate and acetate as examples were performed (Figure 4). For an adequate comparison of

Table 1. Binding constants K_a (M^{-1}) for the formation of 1:1 complexes of **1**–**4** with various anions in [D_6]DMSO/5% $CDCl_3$ at 298 K.[a]

Anion	**1**	**2**	**3**	**4**	pK_a of HX in DMSO (H_2O) [b]	Gas phase basicity (kJ mol^{-1})[c]	Anion volume (Å^3)[d]
$H_2PO_4^-$	2640 ± 610	24700 ± 1070	30000 ± 9500[e]	980 ± 42	– (2.1)	1351	33.5
AcO^-	270 ± 11	7120 ± 1660	23400 ± 5500[e]	380 ± 9	12.6 (4.8)	1427	17.8
F^-	140 ± 15	820 ± 170	6990 ± 1080	35 ± 12	15.0 (3.2)	1529	10.0
HSO_4^-	14 ± 10	15 ± 4	130 ± 37	18 ± 4	– (–3.0)	1251	28.7
$TolSO_3^-$	<5 ± 4	92 ± 7	140 ± 15	14 ± 8	– (–)	–	–
$MeSO_3^-$	13 ± 8	140 ± 6	150 ± 34	25 ± 7	1.6 (–2.6)	1318	–
Cl^-	15 ± 4	88 ± 26	4010 ± 480	42 ± 2	1.8 (–8.0)	1373	24.8
NO_3^-	22 ± 13	<5 ± 10	200 ± 56	29 ± 11	– (–1.3)	1357	24.0
Br^-	20 ± 7	16 ± 15	460 ± 31	27 ± 3	0.9 (–9.0)	1332	31.5
I^-	–[f]	–[f]	220 ± 51	–[f]	– (–)	–	38.8
ClO_4^-	–[f]	–[f]	–[f]	–[f]	– (–10.0)	1180	57.9

[a] The association constants K_a [M^{-1}] were measured by using ^{1}H NMR spectroscopic titrations. The R_2 values for the curve fits used to determine the affinity constants range between 0.974 and 0.999. The anions were used as their tetrabutylammonium salts. [b] Taken from refs.[3e,20] [c] Standard free enthalpy of protonation in the gas phase, taken from refs.[3e,21] [d] Taken from refs.[1i,3f] [e] A host concentration of 2.5×10^{-4} M was used for titration studies, because of the high binding constants.[22] [f] The value of $\Delta\delta_{max}$ was too low for reasonable calculations of K_a.

the binding constants, only the shifts of the amide proton of the azole amide group were used for the calculation of K_a. The maximum shifts $\Delta\delta_{max}$ of these protons after adding 10 equiv. of the guests to the hosts are listed in Table 2. In almost all cases these chemical shifts were the maximum shifted ones. Typical titration curves of **1**–**4** with selected anions are shown in Figures 5, 6, 7 and 8.

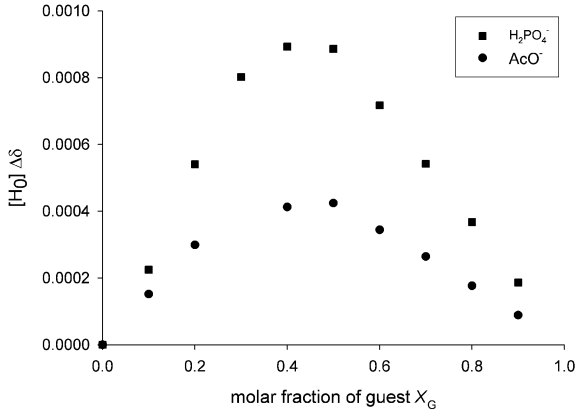

Figure 4. Job plots for complexation of receptor **3** with tetrabutylammonium salts of acetate and dihydrogen phosphate in [D_6]DMSO/5% $CDCl_3$.

Table 2. Values for $\Delta\delta_{max}$ observed by repeated titrations between the anionic guests and receptors **1**–**4** for the amide proton of the azole amide group.

Anion	1	2	3	4
$H_2PO_4^-$	0.905	2.075	1.446	0.583
AcO^-	1.094	1.798	1.295	0.458
F^-	0.803	1.422	1.389	0.231
HSO_4^-	0.031	0.209	0.189	0.044
$TolSO_3^-$	0.043	0.390	0.222	0.052
$MeSO_3^-$	0.050	0.564	0.222	0.067
Cl^-	0.067	0.131	1.759	0.093
NO_3^-	0.023	0.058	0.255	0.044
Br^-	0.027	0.041	0.996	0.080
I^-	0.016	0.026	0.174	0.010
ClO_4^-	0.006	0.022	0.040	–[a]

[a] No shift was observed.

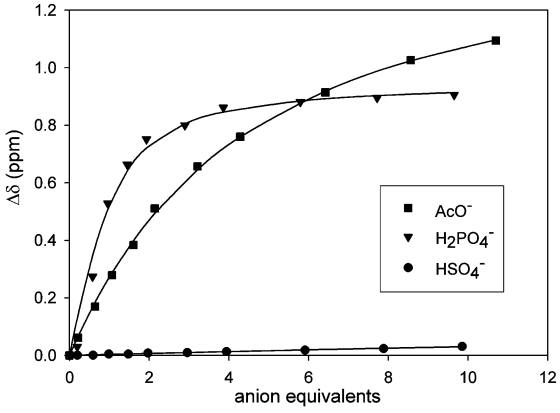

Figure 5. ^{1}H NMR titration curves for the complexation of **1** with tetrabutylammonium salts of acetate, dihydrogen phosphate and hydrogen sulfate in [D_6]DMSO/5% $CDCl_3$.

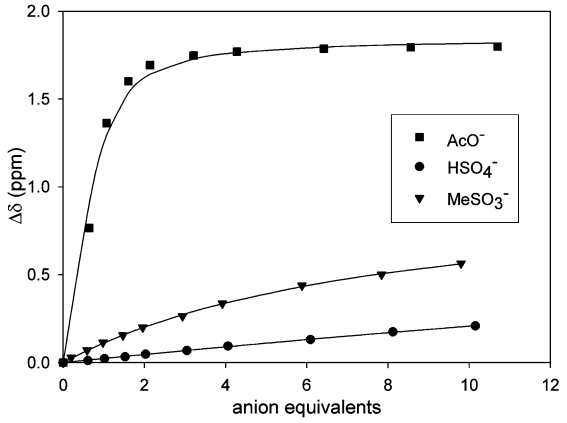

Figure 6. ^{1}H NMR titration curves for the complexation of **2** with tetrabutylammonium salts of acetate, hydrogen sulfate and methyl sulfonate in [D_6]DMSO/5% $CDCl_3$.

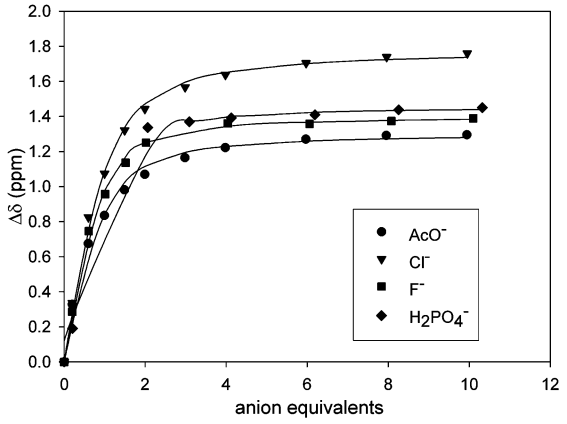

Figure 7. ^{1}H NMR titration curves for the complexation of **3** with tetrabutylammonium salts of acetate, chloride, fluoride and dihydrogen phosphate in [D_6]DMSO/5% $CDCl_3$.

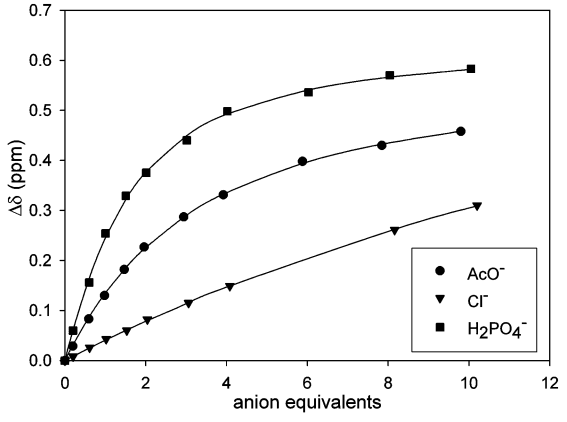

Figure 8. ^{1}H NMR titration curves for the complexation of **4** with tetrabutylammonium salts of acetate, chloride, and dihydrogen phosphate in [D_6]DMSO/5% $CDCl_3$.

Initially, the spherical halides were evaluated. The addition of I^- to receptors **1**, **2** and **4** resulted in only minimal and inconstant downfield shifts of 0.01–0.026 ppm, so that no binding constant could be calculated. By adding

10 equiv. of iodide to **3**, the amide proton shifted about 0.174 ppm and K_a was estimated to be 220 M^{-1}. Comparable results were obtained for the interaction of Br^- and Cl^- with **1**, **2** and **4**. The values for $\Delta\delta_{max}$ are rather small (0.027–0.131 ppm), and the binding constants are in a range 15–88 M^{-1}. A different behaviour is observed for thiazole receptor **3**. Here, shifts of the amide proton of 0.996 and 1.759 ppm for Br^- and Cl^-, respectively, occurred. The binding constant K_a was calculated to be 460 M^{-1} for bromide and 4010 M^{-1} for chloride. The progression of the titration curves shows that after adding approximately 2 equiv. of the guests, the curves fade into a plateau and saturation of the host begins to arise (Figure 7).

The addition of F^- caused in all cases reasonable shifts between 0.231 and 1.422 ppm. Here again, the highest binding constant (7000 M^{-1}) was observed for the interaction with receptor **3**; the titration curve shows that after 1.5 equiv. of fluoride, saturation of the host begins to arise.

If the binding constants of the different receptors are compared with each other a general tendency is seen. Both imidazole receptors **1** and **4** deliver the lowest values for K_a, followed by oxazole receptor **2**. Thiazole receptor **3** shows the highest binding constants for all halides. The comparatively low K_a values for the imidazole receptors can be easily explained. The imidazole is the most basic azole unit and, consequently, when approaching the binding sites, the anions are exposed a much higher repulsion by the lone pairs of the imidazole nitrogen atoms than in the case of the thiazole and the oxazole rings. The fact that the oxazole receptor with the lowest basicity nevertheless has lower binding constants than the thiazole receptor cannot be explained by the basic character of the azole units.

A comparison of the binding constant of complexes **1**–**3**·X^- reveals the relationship between the binding constant and the volume of the halide anions (Table 1). The small fluoride ion binds better than the bigger chloride ion and this in turn interacts stronger than the bromide, whereas for the bulky iodide ion, very weak binding, if at all, can be observed. The reason for this trend is obvious: The small fluoride fits best into the interior of receptors **1**–**3** (Figure 9: molecular structure of **3**·F^- calculated by using B3LYP/6-31G*). An enlargement of the interior of the cyclic peptide leads to a revision of this selectivity. In the case of receptor **4** the hollow space is increased relative to that of receptors **1**–**3**, and therefore, the chloride fits better than the fluoride anion (Table 1 and Figure 9: molecular structure of **4**·Cl^- calculated by using B3LYP/6-31G*). Worth mentioning is that by adding anions to receptor **4** strong H_{ar} interactions were observed. This can be seen from the values of $\Delta\delta_{max}$ of the aromatic protons extending into the interior of the scaffold, which are in the same range as the ones of the amide protons, which indicates direct contacts of these protons to the guests.[23,24] The other aromatic protons shift only slightly upfield.

After the spherical halides, the trigonal planar and tetrahedral anions ($H_2PO_4^-$, HSO_4^-, AcO^-, $TolSO_3^-$, $MeSO_3^-$, NO_3^- and ClO_4^-) were analyzed. Small-to-medium maximum shifts (0.023–0.564 ppm) in combination with small-to-medium values for the binding constants (<5–200 M^{-1}) were observed for HSO_4^-, $TolSO_3^-$, $MeSO_3^-$ and NO_3^-. In the case of ClO_4^-, the chemical shifts were too low to get reasonable values for K_a. All titration curves show a similar progression. Saturation of the host after adding 10 equiv. of guest was not achieved for any of the guests (Figures 5 and 6).

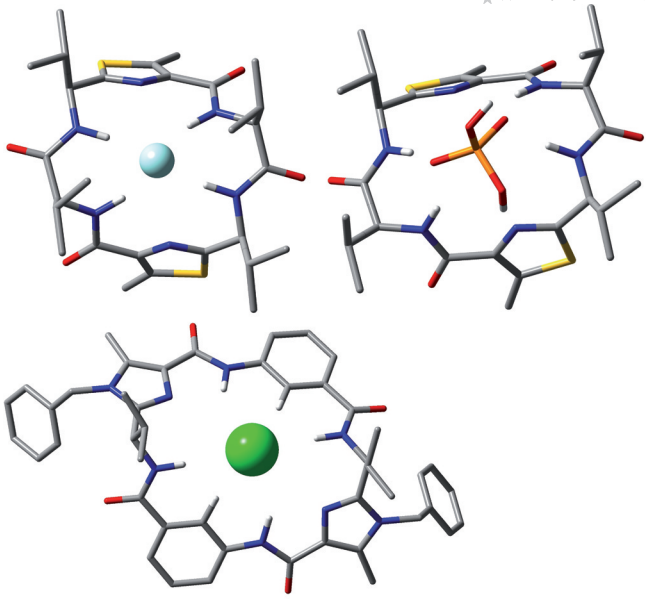

Figure 9. Molecular structures of **3**·F^-, **3**·$H_2PO_4^-$ (above) and **4**·Cl^- (below) calculated by using B3LYP/6-31G*; all hydrogen atoms except those pointing into the interior of the macrocycles are omitted for clarity.

A completely different behaviour was observed for the bonding of AcO^- and $H_2PO_4^-$. By adding acetate, the amide protons reach a maximum shift around 0.458–1.789 ppm. After adding 1.5 equiv. of guest, the titration curves show for **2** and **3** a crossover into a plateau and consequently a saturation of the host (Figures 5–8). The binding constants vary between 270 and 23400 M^{-1} for **1** and **3**, respectively. In the case of the titration with dihydrogen phosphate, the $\Delta\delta_{max}$ value for the NH groups is between 0.583 and 2.075 ppm and the binding constants achieve a maximum value of 30000 M^{-1} for interaction with receptor **3**. Adding one equiv. guest to scaffolds **2** and **3** the curve progression shows saturation (Figure 7). In case of the curves for **1** and **4** the transition is not as straight as that for **2** and **3**, which is due to the smaller binding constants.

A comparison of receptors **1**–**4** shows the same trend that was already found for the halides. The best receptor for all anions is again thiazole receptor **3**, followed by oxazole receptor **2** and imidazole macrocycle **1**. The smallest K_a values are found generally for receptor **4**. Because of the benzene ring, the interior of this receptor is too large to adequately bind the used anions. The complex stability of the individual anions is partially caused by their basicity. The least basic anions like NO_3^-, ClO_4^- and HSO_4^- show the smallest binding constants, whereas acetate and dihydrogen

phosphate, which are more basic than the others, show very high values for K_a.

A general comparison shows that the affinity of the receptors to the anions does not directly depend on the volume of the anions. For example, HSO_4^- and Cl^- adopt different volumes but their binding constants are very similar. In contrast, Br^- and $H_2PO_4^-$ have similar volumes but their values for K_a differ enormously. Even more striking is the comparison of acetate and dihydrogen phosphate: although dihydrogen phosphate is almost twice as large as the acetate ion, their binding constants are quite similar for the interaction with **3**. That means that in addition to their volume, the basicity of the different anions is essential for the strength of their binding. As already mentioned, the binding constants for the weakly basic anions are rather low and with rising basicity their values increase. Because of this, the most basic acetate anion should form the most stable complexes, which however is not the case. Here a further criterion comes into play. The protons of the $H_2PO_4^-$ ion are able to form additional hydrogen bonds with the azole nitrogen atom, and so the binding constants are enhanced (Figure 9: molecular structure of **3**·$H_2PO_4^-$ calculated by using B3LYP/6-31G*). The higher the basicity of the azole nitrogen atom, the higher the selectivity for the $H_2PO_4^-$ ion: The less basic thiazole receptor **3** forms strong complexes with $H_2PO_4^-$ (K_a = 30000 M^{-1}) and AcO^- (K_a = 23400 M^{-1}) and, thus, no selectivity can be observed. In contrast, the more basic imidazole receptor **1**, although yielding distinctly smaller overall K_a values for both (2640 M^{-1} for $H_2PO_4^-$ and 270 M^{-1} for AcO^-), it binds $H_2PO_4^-$ with a 10-fold selectivity vis-a-vis acetate. Consequently, by changing the azole unit the selectivity and the affinity for $H_2PO_4^-$ complexation can be controlled.

Conclusions

We were able to synthesize new azole-based C_2-symmetric macrocyclic peptides and evaluated the binding ability towards anions by using ^{1}H NMR titration techniques in [D_6]DMSO/5% $CDCl_3$. On the one hand, we could show that both the basicity of the anions and the basicity of the receptors play an important role in the formation of strong hydrogen bonds in a host–guest complex. On the other hand, the dimension of the interior of the scaffold is essential for selectivity, especially for the spherical halides. With the synthesis of thiazole receptor **3** we were able to design an excellent receptor for $H_2PO_4^-$ und AcO^- ions. However, imidazole receptor **1** shows overall smaller binding constants; thus, its selectivity for $H_2PO_4^-$ is the highest. Variation of the azole units enables us to design receptors that are either selective or have an affinity for specific anions.

Experimental Section

General Remarks: All chemicals were reagent grade and used as purchased. All moisture-sensitive reactions were performed under an inert atmosphere of argon by using distilled dry solvents. Reactions were monitored by TLC analysis by using silica gel 60 F_{254} thin-layer plates. Flash chromatography was carried out on silica gel 60 (230–400 mesh). ^{1}H and ^{13}C NMR spectra were measured with a Bruker Avance DMX 300 and Avance DRX 500 spectrometers. All chemical shifts (δ) are given in ppm relative to TMS. The spectra were referenced to deuterated solvents indicated in brackets in the analytical data. HRMS spectra were recorded with a Bruker BioTOF III Instrument. IR spectra were measured with a Varian 3100 FTIR Excalibur Series spectrometer. UV/Vis absorption spectra were obtained with a Varian Cary 300 Bio.

Abbreviations: Bn: benzyl; Boc: *tert*-butyloxycarbonyl; FDPP: pentafluorophenyl diphenylphosphinate; DCM: dichloromethane; DMF: *N*,*N*-dimethylformamide; THF: tetrahydrofuran; TFA: trifluoroacetic acid; Val: valine.

Boc-Oxazole Carboxylic Acid 6b: Oxazole **5b** (750 mg, 2.40 mmol) was dissolved in a mixture of methanol (36 mL) and dioxane (24 mL) followed by slow addition of 2 M NaOH solution (12 mL, 24.00 mmol) at 0 °C. The ice bath was removed and stirring was continued overnight. After TLC showed consumption of all starting material, the solution was poured into a mixture of ice (100 g) and DCM (100 mL) and acidified with 2 M HCl to pH = 1. The layers were separated, and the aqueous layer was then repeatedly extracted with DCM (3 × 100 mL). The organic layers were combined, dried with $MgSO_4$ and concentrated in vacuo to give 707 mg (98.8%) of free acid **6b**, which was used without further purification for the next step. ^{1}H NMR (500 MHz, CD_3OD): δ = 4.52 [d, $^3J_{H,H}$ = 7.4 Hz, 1 H, Val α-***CH***], 2.60 (s, 3 H, oxazole-***CH***$_3$), 2.19–2.12 (m, 1 H, Val β-***CH***), 1.44 (s, 9 H, Boc ***CH***$_3$), 0.97 (d, $^3J_{H,H}$ = 6.7 Hz, 3 H, Val ***CH***$_3$), 0.88 (d, $^3J_{H,H}$ = 6.8 Hz, 3 H, Val ***CH***$_3$) ppm. ^{13}C NMR (125 MHz, CD_3OD): δ = 164.9 (q, ***CO***$_2$***H***), 163.8 (q, oxazole ***C***-5), 157.9 (q, Boc ***CONH***), 157.5, (q, oxazole ***C***-2), 128.5 (q, oxazole ***C***-3), 80.7 (q, Boc ***C***), 56.4 (t, Val α-***CH***), 33.3 (t, Val β-***CH***), 28.7 (p, Boc ***CH***$_3$), 19.5 (p, Val ***CH***$_3$), 18.9 (p, Val ***CH***$_3$), 12.0 (p, oxazole -***CH***$_3$) ppm. IR (KBr): $\tilde{\nu}$ = 3318, 2975, 2934, 1724, 1628, 1530, 1368, 1248, 1168, 1096, 1043, 1015, 877, 753 cm^{-1}. UV/Vis (MeOH, $c = 4.00 \times 10^{-5}$ mmol mL^{-1}): λ (log ε) = 215 (3.98) nm. HRMS (ESI): calcd. for $C_{14}H_{22}N_2O_5$ [M + Na]$^+$ 321.1421; found 321.1404.

Boc-Thiazole Carboxylic Acid 6c: Thiazole **5c** (1.42 g, 4.30 mmol) was dissolved in a mixture of methanol (65 mL) and dioxane (44 mL) followed by slow addition of 2 M NaOH solution (22 mL, 24.00 mmol) at 0 °C. The ice bath was removed and stirring was continued overnight. After TLC showed consumption of all starting material, the solution was poured onto a mixture of ice (100 g) and DCM (100 mL) and acidified with 2 M HCl to pH = 1. The layers were separated, and the aqueous layer was then repeatedly extracted with DCM (3 × 100 mL). The organic layers were combined, dried with $MgSO_4$ and concentrated in vacuo to give 1.34 g (99.0%) of the free acid **6c**, which was used without further purification for the next step. ^{1}H NMR (500 MHz, $CDCl_3$): δ = 5.17 (d, $^3J_{H,H}$ = 8.1 Hz, 1 H, Boc-***NH***), 4.78 (dd, $^3J_{H,H}$ = 5.9 Hz, $^3J_{H,H}$ = 7.0 Hz, 1 H, Val α-***CH***), 2.77 (s, 3 H, thiazole-***CH***$_3$), 2.37–2.25 (m, 1 H, Val β-***CH***), 1.45 (s, 9 H, Boc ***CH***$_3$), 0.98 (d, $^3J_{H,H}$ = 6.8 Hz, 3 H, Val ***CH***$_3$), 0.93 (d, $^3J_{H,H}$ = 6.8 Hz, 3 H, Val ***CH***$_3$) ppm. ^{13}C NMR (125 MHz, $CDCl_3$): δ = 168.4 (q, thiazole ***C***-5), 162.7 (q, ***CO***$_2$***H***), 155.4 (q, Boc ***CONH***), 145.1, (q, thiazole ***C***-3), 140.2 (q, thiazole ***C***-2), 80.3 (q, Boc ***C***), 57.7 (t, Val α-***CH***), 33.0 (t, Val β-***CH***), 28.3 (p, Boc ***CH***$_3$), 19.3 (p, Val ***CH***$_3$), 17.4 (p, Val ***CH***$_3$), 12.9 (p, thiazole-***CH***$_3$) ppm. IR (KBr): $\tilde{\nu}$ = 3338, 2976, 2933, 2871, 1686, 1519, 1368, 1314, 1279, 1249, 1167, 1016, 941, 741 cm^{-1}. UV/Vis (MeOH, $c = 2.00 \times 10^{-5}$ mmol mL^{-1}): λ (log ε) = 242 (4.21), 305 (3.95), 324 (sh., 3.84) nm. HRMS (ESI): calcd. for $C_{14}H_{22}N_2O_4S$ [M + Na]$^+$ 337.1209; found 337.1192.

Boc-Oxazole *tert*-Butyl Ester 8b: To a solution of acid **6b** (716 mg, 2.40 mmol) and L-valine *tert*-butyl ester hydrochloride (682 mg, 3.25 mmol) dissolved in absolute CH_3CN (80 mL) was added *N*-ethyldiisopropylamine (0.70 g, 5.40 mmol, 0.92 mL, 2.25 equiv.) at room temperature. Then, FDPP (1.25 g, 3.25 mmol) and an additional amount of *N*-ethyldiisopropylamine (0.70 g, 5.40 mmol, 0.92 mL, 2.25 equiv.) was added. The solution was stirred overnight at room temperature, the solvent was evaporated and the residue was resolved in EtOAc (100 mL). The organic layer was washed with water (3 × 30 mL) and brine (1 × 30 mL), dried with $MgSO_4$ and concentrated, and the residue was subjected to column chromatography on silica gel (*n*-hexane/EtOAc, 2:1) to obtain 1.03 g (94.2%) of **8b** as a white solid. TLC: R_f = 0.52 (*n*-hexane/EtOAc, 3:1; silica). ^{1}H NMR (500 MHz, $CDCl_3$): δ = 7.38 (d, $^3J_{H,H}$ = 9.2 Hz, 1 H, oxazole-*CO*-*NH*), 5.11 (d, $^3J_{H,H}$ = 8.9 Hz, 1 H, Boc-*NH*), 4.69 (dd, $^3J_{H,H}$ = 6.5 Hz, $^3J_{H,H}$ = 8.7 Hz, 1 H, Boc-Val α-*CH*), 4.54 (dd, $^3J_{H,H}$ = 4.7 Hz, $^3J_{H,H}$ = 9.2 Hz, 1 H, oxazole-Val α-*CH*), 2.59 (s, 3 H, oxazole-*CH*$_3$), 2.27–2.19 (m, 1 H, Boc-Val β-*CH*), 2.19–2.10 (m, 1 H, oxazole-Val β-*CH*), 1.48 (s, 9 H, Boc *CH*$_3$), 1.46 (s, 1 H, *tert*-butyl *CH*$_3$), 0.99 (d, $^3J_{H,H}$ = 6.6 Hz, 3 H, Val *CH*$_3$), 0.97 (d, $^3J_{H,H}$ = 6.5 Hz, 3 H, Val *CH*$_3$), 0.94 (d, $^3J_{H,H}$ = 6.5 Hz, 3 H, Val *CH*$_3$), 0.92 (d, $^3J_{H,H}$ = 6.9 Hz, 3 H, Val *CH*$_3$) ppm. ^{13}C NMR (125 MHz, $CDCl_3$): δ = 170.9 (q, *tert*-butyl ***COO***), 161.8 (q, oxazole ***C***-5), 160.7 (q, oxazole-***CONH***), 155.4 (q, Boc ***CONH***), 153.1 (q, oxazole ***C***-2), 128.7 (q, oxazole ***C***-3), 82.0 (q, *tert*-butyl ***C***), 80.1 (q, Boc ***C***), 57.1 (t, Boc-Val α-***CH***), 54.1 (t, oxazole-Val α-***CH***), 32.7 (t, Boc- Val β-***CH***), 31.7 (t, oxazole-Val β-***CH***), 28.3 (p, Boc ***CH***$_3$), 28.0 (p, *tert*-butyl ***CH***$_3$), 19.0 (p, Val ***CH***$_3$), 19.7 (p, Val ***CH***$_3$), 17.9 (p, Val ***CH***$_3$), 17.8 (p, Val ***CH***$_3$), 11.6 (p, oxazole-***CH***$_3$) ppm. IR (KBr): $\tilde{\nu}$ = 3369, 3313, 2972, 2937, 2875, 1719, 1690, 1666, 1636, 1519, 1394, 1370, 1144, 1043, 976, 875 cm^{-1}. UV/Vis (MeOH, $c = 2.00 \times 10^{-5}$ mmol mL^{-1}): λ (log ε) = 222 (4.18) nm. HRMS (FAB): calcd. for $C_{23}H_{39}N_3O_6$ [M + Na]$^+$ 454.2912; found 454.2929. HRMS (FAB): calcd. for $C_{23}H_{39}N_3O_6$ [M – $C_4H_8^+$] 398.2286; found 398.2257.

Boc-Thiazole *tert*-Butyl Ester 8c: To a solution of acid **6c** (690 mg, 2.20 mmol) and L-valine *tert*-butyl ester hydrochloride (620 mg, 2.98 mmol) dissolved in absolute CH_3CN (90 mL) was added *N*-ethyldiisopropylamine (0.64 g, 4.95 mmol, 0.84 mL, 2.25 equiv.) at room temperature. Then, FDPP (1.25 g, 3.25 mmol) and an additional amount of *N*-ethyldiisopropylamine (0.64 g, 4.95 mmol, 0.84 mL, 2.25 equiv.) was added. The solution was stirred overnight at room temperature, the solvent was evaporated and the residue was resolved in EtOAc (100 mL). The organic layer was washed with water (3 × 30 mL) and brine (1 × 30 mL), dried with $MgSO_4$ and concentrated, and the residue was subjected to column chromatography on silica gel (*n*-hexane/EtOAc, 3:1) to obtain 1.02 g (98.2%) of **8c** as a slightly brown solid. TLC: R_f = 0.46 (*n*-hexane/EtOAc, 3:1; silica). ^{1}H NMR (500 MHz, $CDCl_3$): δ = 7.86 (d, $^3J_{H,H}$ = 9.2 Hz, 1 H, thiazole-*CO*-*NH*), 5.11 (d, $^3J_{H,H}$ = 8.6 Hz, 1 H, Boc-*NH*), 4.76 (dd, $^3J_{H,H}$ = 5.6 Hz, $^3J_{H,H}$ = 8.7 Hz, 1 H, Boc-Val α-*CH*), 4.54 (dd, $^3J_{H,H}$ = 4.7 Hz, $^3J_{H,H}$ = 9.2 Hz, 1 H, thiazole-Val α-*CH*), 2.76 (s, 3 H, thiazole-*CH*$_3$), 2.37–2.28 (m, 1 H, Boc-Val β-*CH*), 2.29–2.20 (m, 1 H, thiazole-Val β-*CH*), 1.48 (s, 9 H, Boc *CH*$_3$), 1.46 (s, 9 H, *tert*-butyl *CH*$_3$), 0.99 (d, $^3J_{H,H}$ = 7.0 Hz, 3 H, Val *CH*$_3$), 0.99 (d, $^3J_{H,H}$ = 6.7 Hz, 3 H, Val *CH*$_3$), 0.98 (d, $^3J_{H,H}$ = 7.0 Hz, 3 H, Val *CH*$_3$), 0.93 (d, $^3J_{H,H}$ = 6.8 Hz, 3 H, Val *CH*$_3$) ppm. ^{13}C NMR (125 MHz, $CDCl_3$): δ = 170.9 (q, *tert*-butyl ***COO***), 167.1 (q, thiazole ***C***-5), 162.5 (q, thiazole-***CONH***), 155.5 (q, Boc ***CONH***), 142.4 (q, thiazole ***C***-3), 140.7 (q, thiazole ***C***-2), 81.9 (q, *tert*-butyl ***C***), 80.2 (q, Boc ***C***), 57.6 (t, Boc-Val α-***CH***), 57.3 (t, thiazole-Val α-***CH***), 33.0 (t, Boc-Val β-***CH***), 31.7 (t, thiazole-Val β-***CH***), 28.3 (p, Boc ***CH***$_3$), 28.1 (p, *tert*-butyl ***CH***$_3$), 19.3 (p, Val ***CH***$_3$), 19.0 (p, Val ***CH***$_3$), 17.8 (p, Val ***CH***$_3$), 17.4 (p, Val ***CH***$_3$), 12.6 (p, thiazole-***CH***$_3$) ppm. IR (KBr): $\tilde{\nu}$ = 3573, 3408, 3286, 2969, 2933, 2876, 1728, 1694, 1655, 1519, 1465, 1393, 1369, 1296, 1243, 1166, 1146, 997 cm^{-1}. UV/Vis (MeOH, $c = 2.00 \times 10^{-5}$ mmol mL^{-1}): λ (log ε) = 226 (4.25), 244 (sh., 4.20), 306 (3.77), 326 (sh., 3.63) nm. HRMS (ESI): calcd. for $C_{23}H_{39}N_3O_5S$ [M + H]$^+$ 470.2683; found 470.2712. HRMS (ESI): calcd. for $C_{23}H_{39}N_3O_5S$ [M + Na]$^+$ 492.2530; found 492.2520.

Oxazole Trifluoroacetate 9b: Ester **8b** (500 mg, 1.10 mmol) was dissolved in absolute DCM (10 mL) and cooled to 0 °C. TFA (2.50 g, 22.00 mmol, 1.63 mL) was added slowly, and the reaction mixture was warmed up to room temperature and stirred for another 24 h. Then, the solvent was evaporated, and the residue was stripped several times to remove the remaining TFA to provide 453 mg (100.0%) of trifluoroacetate **9b** as a dark-brown sticky solid. ^{1}H NMR (500 MHz, CD_3OD): δ = 4.52, (d, $^3J_{H,H}$ = 5.0 Hz, 1 H, oxazole-Val α-*CH*), 4.44 (d, $^3J_{H,H}$ = 6.5 Hz, Val-oxazole α-*CH*), 2.65 (s, 1 H, oxazole-*CH*$_3$), 2.44–2.34 (m, 1 H, Val-oxazole β-*CH*), 2.33–2.25 (m, 1 H, oxazole-Val β-*CH*), 1.13 (d, $^3J_{H,H}$ = 6.9 Hz, 3 H, Val *CH*$_3$), 1.04–0.98 (m, 9 H, Val *CH*$_3$) ppm. ^{13}C NMR (125 MHz, CD_3OD): δ = 174.4 (q, Val -***COOH***), 162.9 (q, oxazole ***C***-5), 158.3 (q, oxazole-***CONH***), 156.3 (q, oxazole ***C***-2), 130.3 (q, oxazole ***C***-3), 58.9 (t, oxazole-Val α-***CH***), 58.3 (t, Val-oxazole α-***CH***), 32.5 (t, Val-oxazole β-***CH***), 32.4 (t, oxazole-Val β-***CH***), 19.5 (p, Val ***CH***$_3$), 18.7 (p, Val ***CH***$_3$), 18.2 (p, Val ***CH***$_3$), 18.1 (p, Val ***CH***$_3$), 11.7 (p, oxazole-***CH***$_3$) ppm. IR (KBr): $\tilde{\nu}$ = 3403, 2970, 2937, 1733, 1661, 1531, 1519, 1372, 1195, 1150, 1015, 996, 980 cm^{-1}. UV/Vis (MeOH, $c = 4.00 \times 10^{-5}$ mmol mL^{-1}): λ (log ε) = 222 (4.15) nm. HRMS (ESI): calcd. for $C_{14}H_{23}N_3O_4$ [M + H]$^+$ 298.1761; found 298.1764. HRMS (ESI): calcd. for $C_{14}H_{23}N_3O_3S$ [M + Na]$^+$ 320.1581; found 320.1574.

Thiazole Hydrochloride Salt 9c: Ester **8c** (860 mg, 1.83 mmol) was dissolved in EtOAc (50 mL), cooled down to 0 °C and a saturated solution of HCl in EtOAc (150 mL) was added slowly. After 30 min, the ice bath was removed and stirring was continued at room temperature for an additional 24 h. To remove HCl, argon was bubbled through the solution for 30 min, and then the solvent was evaporated. The residue was stripped several times with EtOAc to provide 637 mg (99.4%) of hydrochloride salt **9c** as a yellow-brown, slightly sticky solid, which was used without further purification for the next step. ^{1}H NMR (500 MHz, CD_3OD): δ = 4.60 (d, $^3J_{H,H}$ = 6.3 Hz, 1 H, Val-thiazole α-*CH*), 4.53 (d, $^3J_{H,H}$ = 5.0 Hz, 1 H, thiazole-Val α-*CH*), 2.81 (s, 3 H, thiazole-*CH*$_3$), 2.41–2.32 (m, 1 H, Val-thiazole β-*CH*), 2.34–2.26 (m, 1 H, thiazole-Val β-*CH*), 1.12 (d, $^3J_{H,H}$ = 6.9 Hz, 3 H, Val *CH*$_3$), 1.06–1.02 (m, 9 H, Val *CH*$_3$) ppm. ^{13}C NMR (125 MHz, CD_3OD): δ = 174.6 (q, Val -***COOH***), 163.6 (q, thiazole ***C***-5), 161.3 (q, thiazole-***CONH***), 144.5 (q, thiazole ***C***-3), 143.3 (q, thiazole ***C***-2), 58.4 (t, Val α-***CH***), 58.3 (t, thiazole-Val α-***CH***), 33.6 (t, Val β-***CH***), 32.1 (t, thiazole-Val β-***CH***), 19.4 (p, Val ***CH***$_3$), 18.4 (p, Val ***CH***$_3$), 18.3 (p, Val ***CH***$_3$), 18.1 (p, Val ***CH***$_3$), 12.5 (p, thiazole-***CH***$_3$) ppm. IR (KBr): $\tilde{\nu}$ = 3376, 2967, 2936, 1715, 1647, 1533, 1515, 1394, 1231, 1114, 995, 979 cm^{-1}. UV/Vis (MeOH, $c = 2.00 \times 10^{-5}$ mmol mL^{-1}): λ (log ε) = 203 (4.10), 228 (3.90), 352 (sh., 3.82) nm. HRMS (ESI): calcd. for $C_{14}H_{23}N_3O_3S$ [M + H]$^+$ 314.1533; found 314.1559. HRMS (ESI): calcd. for $C_{14}H_{23}N_3O_3S$ [M + Na]$^+$ 336.1352; found 336.1377.

Oxazole Receptor 2: To a solution of trifluoroacetate **9b** (453 mg, 1.10 mmol) in anhydrous CH_3CN (50 mL) was added *i*Pr_2NEt (569 mg, 4.40 mmol, 750 μL) at 0 °C followed by the addition of FDPP (634 mg, 1.65 mmol). The solution was warmed up to room temperature and stirred for another 5 d. The solvent was evaporated, the residue was taken up in EtOAc (150 mL) and then

washed with H_2O (3 × 50 mL) and brine (1 × 50 mL). The organic layer was dried with $MgSO_4$ and concentrated. The residue was subjected to column chromatography on silica gel (DCM/EtOAc/MeOH, 75:25:1 → 75:25:2) to obtain 148 mg (47.3%) of receptor **2** as a slightly yellow solid. TLC: R_f = 0.14 (DCM/EtOAc/MeOH, 75:25:2; silica). ^{1}H NMR (500 MHz, $CDCl_3$): δ = 7.00 (d, $^3J_{H,H}$ = 10.3 Hz, 2 H, oxazole-Val *NH*), 6.71 (d, $^3J_{H,H}$ = 7.2 Hz, 2 H, Val-oxazole *NH*), 4.91 (dd, $^3J_{H,H}$ = 6.3 Hz, $^3J_{H,H}$ = 6.9 Hz, 2 H, Val-oxazole α-*CH*), 4.61 (dd, $^3J_{H,H}$ = 7.3 Hz, $^3J_{H,H}$ = 10.3 Hz, 2 H, oxazole-Val α-*CH*), 2.58 (s, 6 H, oxazole-CH_3), 2.42–2.32 (m, 2 H, Val-oxazole β-*CH*), 2.32–2.23 (m, 2 H, oxazole-Val β-*CH*), 1.10 (d, $^3J_{H,H}$ = 6.7 Hz, 6 H, Val CH_3), 1.06 (d, $^3J_{H,H}$ = 6.7 Hz, 6 H, Val CH_3), 1.02 (d, $^3J_{H,H}$ = 6.9 Hz, 6 H, Val CH_3), 0.93 (d, $^3J_{H,H}$ = 6.8 Hz, 6 H, Val CH_3) ppm. ^{13}C NMR (125 MHz, $CDCl_3$): δ = 170.4 (q, *CO*-*NH*-Val), 161.3 (q, oxazole *C*-5), 161.0 (q, oxazole-*CONH*), 154.0 (q, oxazole *C*-2), 128.5 (q, oxazole *C*-3), 59.1 (t, oxazole-Val α-*CH*), 53.3 (t, Val-oxazole α-*CH*), 32.3 (t, Val-oxazole β-*CH*), 31.2 (t, oxazole-Val β-*CH*), 19.4 (p, Val CH_3), 18.8 (p, Val CH_3), 18.3 (p, Val CH_3), 17.8 (p, Val CH_3), 11.6 (p, oxazole-CH_3) ppm. IR (KBr): $\tilde{\nu}$ = 3382, 3322, 2964, 2925, 1655, 1522, 1468, 1189 cm^{-1}. UV/Vis (CH_2Cl_2, $c = 2.00 \times 10^{-5}$ mmol mL^{-1}): λ (log ε) = 217 (4.31) nm. HRMS (ESI): calcd. for $C_{28}H_{42}N_6O_6$ [M + H]$^+$ 559.3239; found 559.3264. HRMS (ESI): calcd. for $C_{23}H_{39}N_3O_5S$ [M + Na]$^+$ 581.3058; found 581.3046.

Thiazole Receptor 3: To a solution of hydrochloride **9c** (658 mg, 1.88 mmol) in anhydrous CH_3CN (95 mL) was added *i*Pr_2NEt (970 mg, 7.52 mmol, 1.28 mL) at 0 °C followed by FDPP (1.08 g, 2.82 mmol). The solution was warmed up to room temperature and stirred for another 5 d. The solvent was evaporated, and the residue was taken up in EtOAc (150 mL) and then washed with H_2O (3 × 50 mL) and brine (1 × 50 mL). The organic layer was dried with $MgSO_4$ and concentrated. The residue was subjected to column chromatography on silica gel (*n*-hexane/EtOAc, 1:3) to obtain 106 mg (19.1%) of scaffold **3** as a white solid. TLC: R_f = 0.14 (*n*-hexane/EtOAc, 1:3; silica). ^{1}H NMR (500 MHz, CD_3OD): δ = 4.80 (d, $^3J_{H,H}$ = 8.5 Hz, 2 H, Val-thiazole α-*CH*), 4.30 (d, $^3J_{H,H}$ = 9.5 Hz, 2 H, thiazole-Val α-*CH*), 2.62 (s, 6 H, thiazole-CH_3), 2.46–2.34 (m, 2 H, Val-thiazole β-*CH*), 2.22–2.11 (m, 2 H, thiazole-Val β-*CH*), 1.10 (d, $^3J_{H,H}$ = 6.7 Hz, 12 H, Val CH_3), 1.05 (d, $^3J_{H,H}$ = 6.7 Hz, 6 H, Val CH_3), 0.91 (d, $^3J_{H,H}$ = 6.7 Hz, 6 H, Val CH_3) ppm. ^{13}C NMR (125 MHz, CD_3OD): δ = 173.3 (q, *CO*-*NH*-Val), 165.7 (q, thiazole *C*-5), 163.8 (q, thiazole-*CONH*), 143.4 (q, thiazole *C*-3), 142.9 (q, thiazole *C*-2), 62.1 (t, Val-thiazole α-*CH*), 57.8 (t, thiazole-Val α-*CH*), 34.7 (t, Val-thiazole β-*CH*), 32.2 (t, thiazole-Val β-*CH*), 20.0 (p, Val CH_3), 19.9 (p, Val CH_3), 19.9 (p, Val CH_3), 19.9 (p, Val CH_3), 12.6 (p, thiazole-CH_3) ppm. IR (KBr): $\tilde{\nu}$ = 3467, 3414, 2966, 2933, 2874, 1655, 1545, 1499, 1467, 1167, 1104, 1075 cm^{-1}. UV/Vis (CH_2Cl_2, $c = 2.00 \times 10^{-5}$ mmol mL^{-1}): λ (log ε) = 229 (sh., 4.14), 244 (4.20) nm. HRMS (ESI): calcd. for $C_{28}H_{42}N_6O_4S_2$ [M + Na]$^+$ 613.2601; found 613.2657. HRMS (ESI): calcd. for $C_{28}H_{42}N_6O_4S_2$ [2M + Na]$^+$ 1203.5310; found 1203.5442. HRMS (ESI): calcd. for $C_{28}H_{42}N_6O_4S_2$ [3M + Na]$^+$ 1794.8047; found 1794.8248.

Boc-Aminobenzoate 11: To a solution of **6a** (980 mg, 2.50 mmol) and methyl 3-aminobenzoate (1.14 g, 7.50 mmol) dissolved in absolute CH_3CN (75 mL) was added *N*-ethyldiisopropylamine (0.98 g, 7.50 mmol, 1.30 mL) at room temperature within 10 min. Then, a suspension of FDPP (1.44 g, 3.75 mmol) in absolute CH_3CN (10 mL) was added slowly. The solution was stirred for 7 d at room temperature, and the solvent was then evaporated. The residue was dissolved in EtOAc (100 mL). The organic layer was washed with water (2 × 30 mL) and brine (1 × 30 mL), dried with $MgSO_4$ and concentrated. The residue was subjected to column chromatography on silica gel (*n*-hexane/EtOAc, 2:1) to obtain 533 mg (40.8%) **11** as a white solid. TLC: R_f = 0.30 (*n*-hexane/EtOAc, 2:1; silica). ^{1}H NMR (500 MHz, $CDCl_3$): δ = 9.16 (s, 1 H, imidazole -*CO*-*NH*), 8.18 (m, 1 H, H_{ar}), 8.12–8.11 (m, 1 H, H_{ar}), 7.78–7.76 (m, 1 H, H_{ar}), 7.44–7.41 (m, 1 H, H_{ar}), 7.33–7.27 (m, 3 H, H_{ar}), 7.02–7.00 (m, 2 H, H_{ar}), 5.30 (d, $^2J_{H,H}$ = 16.8 Hz, 1 H, CH_2), 5.17 (d, $^2J_{H,H}$ = 16.8 Hz, 1 H, CH_2), 4.98 (d, $^3J_{H,H}$ = 9.7 Hz, 1 H, Boc-*NH*), 4.54–4.50 (m, 1 H, Boc-Val α-*CH*), 3.93 (s, 3 H, CO_2CH_3), 2.56 (s, 3 H, imidazole-CH_3), 2.23–2.16 (m, 1 H, Boc-Val β-*CH*), 1.39 (s, 9 H, Boc CH_3), 0.98 (d, $^3J_{H,H}$ = 6.6 Hz, 3 H, Val CH_3), 0.71 (d, $^3J_{H,H}$ = 6.6 Hz, 3 H, Val CH_3) ppm. ^{13}C NMR (125 MHz, $CDCl_3$): δ = 166.95 (q, methyl *COO*), 162.00 (q, imidazole-*CONH*), 155.37 (q, Boc *CONH*), 147.35 (q, imidazole *C*-5), 138.64 (q, C_{ar}), 135.68 (q, imidazole *C*-3), 133.60 (q, C_{ar}), 130.80 (q, C_{ar}), 129.93 (q, imidazole *C*-2), 129.09 (t, C_{ar}), 128.96 (t, C_{ar}), 127.89 (t, C_{ar}), 126.05 (t, C_{ar}), 124.54 (t, C_{ar}), 123.86 (t, C_{ar}), 120.24 (t, C_{ar}), 79.74 (q, Boc *C*), 52.18 (p, CO_2CH_3), 51.99 (t, Boc-Val α-*CH*), 46.71 (s, CH_2), 32.63 (t, Boc-Val β-*CH*), 28.29 (p, Boc CH_3), 19.81 (p, Val CH_3), 18.32 (p, Val CH_3), 10.00 (p, imidazole-CH_3) ppm. IR (KBr): $\tilde{\nu}$ = 3348, 3000, 1724, 1644 cm^{-1}. UV/Vis (MeOH, $c = 3.22 \times 10^{-5}$ mmol mL^{-1}): λ (log ε) = 271 (4.36) nm. HRMS (ESI): calcd. for $C_{28}H_{37}N_4O_5$ [M + H]$^+$ 521.2758; found 521.2763. HRMS (ESI): calcd. for $C_{28}H_{37}N_4O_5$ [M + Na]$^+$ 543.2578; found 543.2583. HRMS (ESI): calcd. for $C_{28}H_{37}N_4O_5$ [2M + H]$^+$ 1041.5444; found 1041.5464. HRMS (ESI): calcd. for $C_{28}H_{37}N_4O_5$ [2M + Na]$^+$ 1063.5264; found 1063.5285.

Boc-Aminobenzoic Acid 12: Ester **11** (130 mg, 0.25 mmol) was dissolved in a mixture of methanol (6.0 mL) and dioxane (6.0 mL) followed by the slow addition of 2 M NaOH solution (1.25 mL, 2.50 mmol) at 0 °C. The ice bath was removed and stirring was continued overnight. After TLC showed consumption of all starting material, the solution was poured into a mixture of ice (20 g) and DCM (20 mL) and acidified with 2 M HCl to pH = 1. The layers were separated, and the aqueous layer was then repeatedly extracted with DCM (3 × 100 mL). The organic layers were combined, dried with $MgSO_4$ and concentrated in vacuo to give 126 mg (100.0%) of free acid **12**, which was used without further purification for the next step. ^{1}H NMR (500 MHz, $CDCl_3$): δ = 8.95 (s, 1 H, imidazole -*CO*-*NH*), 8.62 (m, 1 H, H_{ar}), 8.04 (m, 1 H, H_{ar}), 7.92–7.90 (m, 1 H, H_{ar}), 7.49–7.46 (m, 1 H, H_{ar}), 7.37–7.30 (m, 3 H, H_{ar}), 7.10–7.09 (m, 2 H, H_{ar}), 5.58 (d, $^2J_{H,H}$ = 16.8 Hz, 1 H, CH_2), 5.24 (d, $^2J_{H,H}$ = 16.8 Hz, 1 H, CH_2), 4.60–4.56 (m, 1 H, Boc-Val α-*CH*), 2.66 (s, 3 H, imidazole-CH_3), 2.40–2.30 (m, 1 H, Boc-Val β-*CH*), 1.45 (s, 9 H, Boc CH_3), 0.99 (d, $^3J_{H,H}$ = 6.5 Hz, 3 H, Val CH_3), 0.54 (d, $^3J_{H,H}$ = 6.5 Hz, 3 H, Val CH_3) ppm. ^{13}C NMR (125 MHz, $CDCl_3$): δ = 168.77 (q, methyl *COOH*), 160.84 (q, imidazole-*CONH*), 156.04 (q, Boc *CONH*), 148.94 (q, imidazole *C*-5), 138.50 (q, C_{ar}), 135.22 (q, imidazole *C*-3), 135.00 (q, C_{ar}), 130.66 (q, C_{ar}), 129.37 (q, imidazole *C*-2), 129.08 (t, C_{ar}), 128.15 (t, C_{ar}), 126.30 (t, C_{ar}), 125.82 (t, C_{ar}), 124.64 (t, C_{ar}), 124.63 (t, C_{ar}), 120.21 (t, C_{ar}), 79.64 (q, Boc *C*), 52.23 (t, Boc-Val α-*CH*), 47.05 (s, CH_2), 32.08 (t, Boc-Val β-*CH*), 28.36 (p, Boc CH_3), 19.90 (p, Val CH_3), 19.23 (p, Val CH_3), 10.26 (p, imidazole-CH_3) ppm. IR (KBr): $\tilde{\nu}$ = 3356, 3000, 1685, 1679 cm^{-1}. UV/Vis (MeOH, $c = 1.66 \times 10^{-5}$ mmol mL^{-1}): λ (log ε) = 272 (4.34) nm. HRMS (ESI): calcd. for $C_{28}H_{34}N_4O_5$ [M + H]$^+$ 507.2602; found 507.2632. HRMS (ESI): calcd. for $C_{28}H_{34}N_4O_5$ [M + Na]$^+$ 529.2421; found 529.2451.

Trifluoroacetate 13: Boc protected amino acid **12** (115 mg, 0.23 mmol) was dissolved in absolute DCM (5 mL) and cooled to 0 °C. TFA (360 μL) was added slowly, and the reaction mixture was warmed up to room temperature and stirring was continued for another 3 h. Then, the solvent was evaporated, and the residue was stripped several times to remove the remaining TFA and to provide

119 mg (100.0%) of trifluoroacetate **13** as a white sticky solid, which was used without further purification for the next step. ^{1}H NMR (500 MHz, [D$_6$]DMSO): δ = 9.77 (s, 1 H, imidazole -*CO*-*NH*), 8.60–8.50 (m, 3 H, *NH*$_3^+$), 8.33–8.32 (m, 1 H, *H*$_{ar}$), 8.03–8.01 (m, 1 H, *H*$_{ar}$), 7.67–7.65 (m, 1 H, *H*$_{ar}$), 7.49–7.46 (m, 1 H, *H*$_{ar}$), 7.40–7.37 (m, 2 H, *H*$_{ar}$), 7.33–7.30 (m, 1 H, *H*$_{ar}$), 7.12–7.10 (m, 2 H, *H*$_{ar}$), 5.42 (d, $^2J_{H,H}$ = 17.1 Hz, 1 H, *CH*$_2$), 5.33 (d, $^2J_{H,H}$ = 17.1 Hz, 1 H, *CH*$_2$), 4.51–4.45 (m, 1 H, Val α-*CH*), 2.41 (s, 3 H, imidazole-*CH*$_3$), 2.23–2.16 (m, 1 H, Val β-*CH*), 0.93 (d, $^3J_{H,H}$ = 6.8 Hz, 3 H, Val *CH*$_3$), 0.82 (d, $^3J_{H,H}$ = 6.8 Hz, 3 H, Val *CH*$_3$) ppm. ^{13}C NMR (125 MHz, [D$_6$]DMSO): δ = 167.05 (q, *COOH*), 161.15 (q, imidazole-*CONH*), 142.88 (q, imidazole *C*-5), 138.74 (q, *C*$_{ar}$), 135.92 (q, imidazole *C*-3), 134.24 (q, *C*$_{ar}$), 131.34 (q, *C*$_{ar}$), 129.62 (q, imidazole *C*-2), 129.02 (t, *C*$_{ar}$), 128.72 (t, *C*$_{ar}$), 127.63 (t, *C*$_{ar}$), 126.28 (t, *C*$_{ar}$), 123.98 (t, *C*$_{ar}$), 123.22 (t, *C*$_{ar}$), 119.88 (t, *C*$_{ar}$), 51.17 (t, Val α-*CH*), 46.41 (s, *CH*$_2$), 31.48 (t, Val β-*CH*), 18.28 (p, Val *CH*$_3$), 17.37 (p, Val *CH*$_3$), 9.60 (p, imidazole-*CH*$_3$) ppm. IR (KBr): $\tilde{\nu}$ = 3375, 3000, 1680, 1679 cm^{-1}. UV/Vis (MeOH, c = 1.96 × 10^{-5} mmol mL^{-1}): λ (log ε) = 268 (4.32) nm. HRMS (ESI): calcd. for $C_{23}H_{26}N_4O_3$ [M + H]$^+$ 407.2078; found 407.2108. HRMS (ESI): calcd. for $C_{23}H_{26}N_4O_3$ [M + Na]$^+$ 429.1897; found 429.1920.

Receptor 4: To a solution of trifluoroacetate **13** (515 mg, 0.99 mmol) in anhydrous CH_3CN (34 mL) was added *i*Pr$_2$NEt (384 mg, 2.97 mmol, 508 μL) at 0 °C followed by FDPP (571 mg, 1.49 mmol). The solution was warmed up to room temperature and stirred for another 7 d. The solvent was evaporated, and the residue was taken up in EtOAc (150 mL) and then washed with H_2O (3 × 50 mL) and brine (1 × 50 mL). The organic layer was dried with $MgSO_4$, filtered and concentrated, and the residue was subjected to column chromatography on silica gel (DCM/EtOAc/MeOH, 75:25:1 → 75:25:5) to obtain 200 mg (52.5%) of receptor **4** as a white solid. TLC: R_f = 0.30 (DCM/EtOAc/MeOH, 75:25:2; silica). ^{1}H NMR (500 MHz, $CDCl_3$): δ = 9.18 (s, 2 H, imidazole -*CO*-*NH*), 8.71–8.70 (m, 2 H, *H*$_{ar}$), 7.80–7.78 (m, 2 H, *H*$_{ar}$), 7.53–7.50 (m, 2 H, *H*$_{ar}$), 7.35–7.30 (m, 8 H, *H*$_{ar}$), 7.15–7.13 (d, $^3J_{H,H}$ = 8.2 Hz, 2 H, *NH*- Val), 7.04–7.03 (m, 4 H, *H*$_{ar}$), 5.44–5.40 (m, 6 H, *CH*$_2$, Val α-*CH*), 2.55 (s, 6 H, imidazole-*CH*$_3$), 2.10–2.04 (m, 2 H, Val β-*CH*), 1.00 (d, $^3J_{H,H}$ = 6.6 Hz, 6 H, Val *CH*$_3$), 0.82 (d, $^3J_{H,H}$ = 6.6 Hz, 6 H, Val *CH*$_3$) ppm. ^{13}C NMR (125 MHz, $CDCl_3$): δ = 165.51 (q, *PhCOONH*), 161.56 (q, imidazole-*CONH*), 147.34 (q, imidazole *C*-5), 138.38 (q, *C*$_{ar}$), 134.96 (q, imidazole *C*-3), 134.00 (q, *C*$_{ar}$), 133.73 (q, *C*$_{ar}$), 130.26 (q, imidazole *C*-2), 130.09 (t, *C*$_{ar}$), 129.18 (t, *C*$_{ar}$), 128.24 (t, *C*$_{ar}$), 126.04 (t, *C*$_{ar}$), 123.86 (t, *C*$_{ar}$), 122.76 (t, *C*$_{ar}$), 115.22 (t, *C*$_{ar}$), 50.81 (t, Val α-*CH*), 47.24 (s, *CH*$_2$), 34.41 (t, Val β-*CH*), 19.40 (p, Val *CH*$_3$), 18.05 (p, Val *CH*$_3$), 10.06 (p, imidazole-*CH*$_3$) ppm. IR (KBr): $\tilde{\nu}$ = 3430, 3378, 3000, 1673, 1679 cm^{-1}. UV/Vis (MeOH, c = 2.78 × 10^{-5} mmol mL^{-1}): λ (log ε) = 270 (4.42) nm. HRMS (ESI): calcd. for $C_{46}H_{48}N_8O_4$ [M + H]$^+$ 777.3871; found 777.3876. HRMS (ESI): calcd. for $C_{46}H_{48}N_8O_4$ [M + Na]$^+$ 799.3691; found 799.3696.

^{1}H NMR Titrations: All salts and ligands were predried under high vacuum and then kept under an atmosphere of argon. [D$_6$]DMSO of 99.9% isotopic purity and $CDCl_3$ of 99.8% isotopic purity, purchased from Sigma–Aldrich, were used as received. For the titration experiments a Bruker Avance DMX 300 (^{1}H: 300 MHz) was used.

For determination of the binding constants, stock solutions of the host molecule being studied were made up in [D$_6$]DMSO/5% $CDCl_3$ with a final concentration of 1.00 × 10^{-3} mmol mL^{-1}. Stock solutions of the anions were prepared by dissolving around 20 equiv. of the TBA salts in 2 mL of the host stock solution.

From this, 10 to 500 μL portions were again diluted with the host stock solution up to 1 mL to receive the samples that were measured. The shifts of the proton signals were monitored and 10 data points were recorded. The association constants were calculated from changes in chemical shifts from the amide protons of the ligands. Nonlinear curve fit for a simple 1:1 binding model was carried out with the SigmaPlot 9.0 program.

For the Job plot titrations, stock solutions of the host molecule and the respective guest molecules were made up in [D$_6$]DMSO/5% $CDCl_3$ with a final concentration of 4 × 10^{-3} mmol mL^{-1}. From the host solution, 100–1000 μL were put into an NMR tube and filled with the guest solution up to 1 mL, so that the sum of the host and guest concentration was constant in each sample. The samples were measured and afterwards analyzed by plotting the molar fraction of guest (X_G) as a function of [H$_0$] × Δδ.[25] The plots themselves were generated by using SigmaPlot 9.0.

Acknowledgments

This work was generously supported by the Deutsche Forschungsgemeinschaft. The authors thank Dr. Andreea Schuster for helpful discussions.

[1] For selected reviews, see: a) P. A. Gale, S. E. Garcia-Garrido, J. Garric, *Chem. Soc. Rev.* **2008**, *37*, 151–190; b) J. L. Sessler, *Coord. Chem. Rev.* **2006**, *250*, 3004–3037; c) C. R. Bondy, S. J. Loeb, *Coord. Chem. Rev.* **2003**, *240*, 77–99; d) T. N. Lambert, B. D. Smith, *Coord. Chem. Rev.* **2003**, *240*, 129–141; e) R. Martinez-Manez, F. Sancenón, *Chem. Rev.* **2003**, *103*, 4419–4476; f) M. D. Best, S. L. Tobey, E. V. Anslyn, *Coord. Chem. Rev.* **2003**, *240*, 3–15; g) A. P. Davis, J.-B. Joos, *Coord. Chem. Rev.* **2003**, *240*, 143–156; h) K. Choi, A. D. Hamilton, *Coord. Chem. Rev.* **2003**, *240*, 101–110; i) F. P. Schmidtchen, M. Berger, *Chem. Rev.* **1997**, *97*, 1609–1646; j) A. Bianchi, K. Bowman-James, E. García-Espana (Eds.), *Supramolecular Chemistry of Anions*, Wiley-VCH, Weinheim, **1997**.

[2] For some recent examples, see: a) A. J. Lowe, G. A. Dyson, F. M. Pfeffer, *Eur. J. Org. Chem.* **2008**, 1559–1567; b) Y. Li, A. H. Flood, *J. Am. Chem. Soc.* **2008**, *130*, 12111–12122; c) O. B. Berryman, A. C. Sather, B. P. Hay, J. S. Meisner, D. W. Johnson, *J. Am. Chem. Soc.* **2008**, *130*, 10895–10897; d) C. Schmuck, V. Bickert, *J. Org. Chem.* **2007**, *72*, 6832–6839; e) F. M. Pfeffer, K. F. Lim, K. J. Sedgwick, *Org. Biomol. Chem.* **2007**, *5*, 1795–1799; f) G. W. Bates, Triyanti, M. E. Light, M. Albrecht, P. A. Gale, *J. Org. Chem.* **2007**, *72*, 8921–8927; g) J. L. Sessler, N. M. Barkey, G. Dan Pantos, V. M. Lynch, *New J. Chem.* **2007**, *31*, 646–654; h) S. Nieto, J. Pérez, L. Riera, D. Miguel, *Chem. Eur. J.* **2006**, *12*, 2244–2251; i) M. Mascal, *Angew. Chem.* **2006**, *118*, 2956–2959; *Angew. Chem. Int. Ed.* **2006**, *45*, 2890–2893; j) K. Navakhun, P. A. Gale, M. B. Hursthouse, *Chem. Commun.* **2002**, 2084–2085.

[3] For some recent examples of cyclopeptide-based anion receptors, see: a) D. Meshcheryakov, F. Arnaud-Neu, V. Böhmer, M. Bolte, V. Hubscher-Bruder, E. Jobin, I. Thondorf, S. Werner, *Org. Biomol. Chem.* **2008**, *6*, 1004–1014; b) S. J. Brooks, S. E. Garcia-Garrido, M. E. Light, P. A. Cole, P. A. Gale, *Chem. Eur. J.* **2007**, *13*, 3320–3329; c) C. Reyheller, B. H. Hay, S. Kubik, *New J. Chem.* **2007**, *31*, 2095–2101; d) S.-W. Kang, C. M. Gothard, S. Maitra, A.-T. Wahab, J. S. Nowick, *J. Am. Chem. Soc.* **2007**, *129*, 1486–1487; e) M. J. Chmielewski, J. Jurczak, *Chem. Eur. J.* **2005**, *11*, 6080–6094; f) J. L. Sessler, V. M. Lynch, Y. A. Ustinyuk, *Org. Lett.* **2005**, *7*, 5277–5280; g) K. Choi, A. D. Hamilton, *J. Am. Chem. Soc.* **2003**, *125*, 10241–10249; h) R. Herges, A. Dikmans, U. Jana, F. Köhler, P. Jones, I. Dix, T. Fricke, B. König, *Eur. J. Org. Chem.* **2002**, 3004–3014; i) D. Ranganathan, *Acc. Chem. Res.* **2001**, *34*, 919–930; j) H. Ishida, M. Suga, K. Donowaki, K. Ohkubo, *J. Org. Chem.* **1995**, *60*, 5374–5375.

[4] a) K. H. Hirsch, F. R. Fischer, F. Diederich, *Angew. Chem.* **2007**, *119*, 342–357; *Angew. Chem. Int. Ed.* **2007**, *46*, 338–352; b) J. L. Sessler, D. Seidel, *Angew. Chem.* **2003**, *115*, 5292–5333; *Angew. Chem. Int. Ed.* **2003**, *42*, 5134–5175; c) P. D. Beer, P. A. Gale, *Angew. Chem.* **2001**. *113*, 502–532; *Angew. Chem. Int. Ed.* **2001**, *40*, 486–516.
[5] a) H. Luecke, F. A. Quiocho, *Nature* **1990**, *347*, 402–406; b) J. J. He, F. A. Quiocho, *Science* **1991**, *251*, 1479–1481; c) B. L. Jacobsen, F. A. Quiocho, *J. Mol. Biol.* **1988**, *204*, 783–787.
[6] D. M. Perreault, X. Chen, E. V. Anslyn, *Tetrahedron* **1995**, *51*, 353–362.
[7] J. W. Steed, J. L. Atwood in *Supramolecular Chemistry*, John Wiley & Sons, Chichester, **2000**.
[8] G. Haberhauer, T. Oeser, F. Rominger, *Chem. Eur. J.* **2005**, *11*, 6718–6726.
[9] G. Haberhauer, *Angew. Chem.* **2007**, *119*, 4476–4479; *Angew. Chem. Int. Ed.* **2007**, *46*, 4397–4399.
[10] G. Haberhauer, *Angew. Chem.* **2008**, *120*, 3691–3694; *Angew. Chem. Int. Ed.* **2008**, *47*, 3635–3638.
[11] G. Haberhauer, T. Oeser, F. Rominger, *Chem. Commun.* **2005**, 2799–2801.
[12] Á. Pintér, G. Haberhauer, *Eur. J. Org. Chem.* **2008**, 2375–2387.
[13] C. A. Hunter, D. H. Purvis, *Angew. Chem.* **1992**, *104*, 779–782.
[14] J. F. Malone, C. M. Murray, G. M. Dolan, A. J. Lavery, *Chem. Mater.* **1997**, *9*, 2983–2989.
[15] M. Karplus, *J. Chem. Phys.* **1959**, *30*, 11–15.
[16] All computations were performed with the Gaussian 03 program-package: M. J. Frisch, G. W. Trucks, H. B. Schlegel, G. E. Scuseria, M. A. Robb, J. R. Cheeseman, J. A. Montgomery Jr, T. Vreven, K. N. Kudin, J. C. Burant, J. M. Millam, S. S. Iyengar, J. Tomasi, V. Barone, B. Mennucci, M. Cossi, G. Scalmani, N. Rega, G. A. Petersson, H. Nakatsuji, M. Hada, M. Ehara, K. Toyota, R. Fukuda, J. Hasegawa, M. Ishida, T. Nakajima, Y. Honda, O. Kitao, H. Nakai, M. Klene, X. Li, J. E. Knox, H. P. Hratchian, J. B. Cross, V. Bakken, C. Adamo, J. Jaramillo, R. Gomperts, R. E. Stratmann, O. Yazyev, A. J. Austin, R. Cammi, C. Pomelli, J. W. Ochterski, P. Y. Ayala, K. Morokuma, G. A. Voth, P. Salvador, J. J. Dannenberg, V. G. Zakrzewski, S. Dapprich, A. D. Daniels, M. C. Strain, O. Farkas, D. K. Malick, A. D. Rabuck, K. Raghavachari, J. B. Foresman, J. V. Ortiz, Q. Cui, A. G. Baboul, S. Clifford, J. Cioslowski, B. B. Stefanov, G. Liu, A. Liashenko, P. Piskorz, I. Komaromi, R. L. Martin, D. J. Fox, T. Keith, M. A. Al-Laham, C. Y. Peng, A. Nanayakkara, M. Challacombe, P. M. W. Gill, B. Johnson, W. Chen, M. W. Wong, C. Gonzalez, J. A. Pople, *Gaussian 03*, Revision C.02, Gaussian, Inc., Wallingford, CT, **2004**.
[17] G. Haberhauer, Á. Pintér, T. Oeser, F. Rominger, *Eur. J. Org. Chem.* **2007**, 1779–1792.
[18] J.-L. Wu, Y.-B. He, Z.-Y. Zeng, L.-H. Wie, L.-Z. Meng, t.-X. Yang, *Tetrahedron* **2004**, *60*, 4309–4314.
[19] C. B. Aakeroy in *Encyclopedia of Supramolecular Chemistry* (Eds: J. L. Atwood, J. W. Steed), Marcel Dekker, New York, **2004**, pp. 1380–1381.
[20] E. Riedel (Ed.), *Anorganische Chemie*, Walter de Gruyter, Berlin, **1994**.
[21] *NIST Chemistry WebBook*, http://webbook.nist.gov/chemistry/.
[22] K. Hirose in *Analytical Methods in Supramolecular Chemistry* (Ed.: C. A. Schalley), Wiley-VCH, Weinheim, **2007**, pp. 17–54.
[23] V. S. Bryantsev, B. P. Hay, *Org. Lett.* **2005**, *7*, 5031–5034.
[24] a) V. S. Bryantsev, B. P. Hay, *J. Am. Chem. Soc.* **2005**, *127*, 8282–8283; b) O. B. Berryman, V. S. Bryantsev, D. P. Stay, D. W. Johnson, B. P. Hay, *J. Am. Chem. Soc.* **2007**, *129*, 48–58.
[25] K. A. Connors (Ed.), *Binding Constants*, John Wiley & Sons, New York, **1987**.

Received: August 22, 2008
Published Online: November 27, 2008

